It is interesting that these findings for the thermal decomposition of DBH are very similar to those obtained by Adams et al.[8] for the photochemical dissociation. The conditions necessary for the collisional thermal decomposition preclude the possibility of analysis of the rotational state of nascent nitrogen. This is unfortunate, since it would be interesting to know whether the N_2 is born rotationally cold, as found by Adams el al. for the photolysis of DBH. The small degree of rotational excitation in the N_2 is unexpected and is in great contrast to recent findings that CO is born with large amounts of rotational excitation in the photochemical dissociation of 3-cyclopentenone and 7-norbornenone.[15]

Registry No. DBH, 2721-32-6; CO, 630-08-0; cyclopentene, 142-29-0.

(15) Jimenez, R.; Kable, S. H.; Loison, J.-C.; Simpson, C. J. S. M.; Adam, W.; Houston, P. L. To be published.

Structure of the Trimethylamine–Sulfur Dioxide Complex

Jung Jin Oh, Marabeth S. LaBarge, Jose Matos, Jeff W. Kampf, Kurt W. Hillig II, and Robert L. Kuczkowski*

Contribution from the Department of Chemistry, University of Michigan, Ann Arbor, Michigan 48109-1055. *Received October 19, 1990*

Abstract: The microwave spectrum of the charge-transfer complex between trimethylamine and sulfur dioxide has been studied with a pulsed molecular beam Fourier transform microwave spectrometer. In addition to the normal isotopic form, the rotational spectra of the $(CH_3)_3N{\cdot}^{34}SO_2$, $(CH_3)_3{}^{15}N{\cdot}SO_2$, $(CH_3)_3N{\cdot}SO^{18}O$, $(CH_3)_3N{\cdot}S^{18}O_2$, and $^{13}CH_3(CH_3)_2N{\cdot}SO_2$ isotopic species were assigned. Stark effect measurements gave electric dipole components of $\mu_a = 4.676$ (5), $\mu_c = 1.081$ (4), and $\mu_{total} = 4.800$ (5) D. The dipole moment and moment of inertia data show that the complex belongs to the C_s point group. The crystal structure of the charge-transfer complex has been reexamined at −70 °C by X-ray crystallography and is in good agreement with an earlier room-temperature determination. The structure of this complex in both the gas and solid phase is consistent with the nitrogen lone pair pointing toward the sulfur atom, with the SO_2 plane tilted by ~75° from the C_3 axis of the trimethylamine. The methyl groups are staggered with respect to the oxygen atoms. In the gas phase, the nitrogen to sulfur distance is 2.26 (3) Å; this distance shortens to 2.05 (1) Å in the crystal. From the dipole moment and the nitrogen nuclear quadrupole coupling constants, an upper limit was estimated for the transfer of charge from the nitrogen to the sulfur atom as 0.2 to 0.3 electron.

Introduction

The trimethylamine–sulfur dioxide ($TMA{\cdot}SO_2$) complex is one of the most thoroughly studied amine·SO_2 charge-transfer complexes.[1] This 1:1 addition compound forms a readily sublimable white solid with a melting point of 77 °C.[2,3] The charge-transfer band of the complex occurs at 276 nm in the gas phase and shows an unusual blue shift upon solvation to 273 nm in heptane and 258 nm in dichloromethane.[4-6] From this absorption feature, as well as from pressure measurements, the reaction thermodynamics were evaluated in the gas phase and in heptane solvent.[5] The solvation energies for the free species and the lattice energy for the complex were also determined, allowing a complete thermodynamic cycle to be constructed. The dissociation energy was found to be 9.1 (4) kcal/mol in the gas phase and 11.0 (5) kcal/mol in heptane. The unusual blue shift and the increased stability upon solvation were explained by strong dipole-induced dipole interactions with the solvent which stabilize the ground state of the complex more than free TMA and SO_2. This was consistent with the large dipole moment of 4.95 (5) D determined for the complex in benzene.[3]

It was proposed from the dipole moment and spectral data that the nitrogen end of TMA points to the plane of the SO_2, as expected for a n(lp)–π^* interaction,[3,5] and this was confirmed when the crystal structure was reported.[7] The C_3 axis of the TMA was essentially colinear with the "N–S bond". The N–S distance was 2.062 (6) Å with a tilt angle of 68° between the SO_2 plane and the N–S axis. This N–S distance, compared to the sum of the van der Waals radii (3.35 Å) and that of the covalent radii (1.74 Å)[8] for nitrogen and sulfur, implied an appreciable interaction and raised questions about possible small structural deformations in each monomer. This question could not be answered definitively because of the uncertainties in the structure analysis although several parameters showed deviations from the monomers. More insight on the interaction was obtained from an IR study of the methyl-substituted amines in argon and nitrogen matrices.[9] A shift in the IR bands of the SO_2 subunit was observed for all the complexes. For the $TMA{\cdot}SO_2$ complex the antisymmetric stretching mode decreased from 1350 cm^{-1} for free SO_2 to 1270

Table I. Previous Structural Studies of $(CH_3)_3N{\cdot}SO_2$

	ref				
	10	11	12, 13	7	17
method	STO-3G	4-31G	3-21G[d]	X-ray	MW
d(N–S), Å[a]	2.86	2.36	2.13	2.06 (1)	2.27 (3)
α, deg	0[b]	0[b]	0[b]	0	19 (5)
β, deg	90[b]	85[b]	81	68	91 (2)
$-\Delta E$, kcal/mol[c]	4.06	14.8[e]	11.3		

[a] See Figure 1 for parameter definitions. [b] Assumed. [c] TMA(g) + SO_2(g) → $TMA{\cdot}SO_2$(g), =9.1 kcal/mol, experimental value.[5] [d] d polarization functions on N and S. [e] At d(N–S) = 2.45 Å.

(1) Tamres, M. *Molecular Complexes*; Foster, R., Ed.; Crane, Russak: New York, NY, 1973; Vol. 1, Chapter 2.
(2) Burg, A. B. *J. Am. Chem. Soc.* **1943**, *65*, 1629.
(3) Moede, J. A.; Curran, C. *J. Am. Chem. Soc.* **1949**, *71*, 852.
(4) Christian, S. D.; Grundnes, J. *Nature (London)* **1967**, *214*, 1111.
(5) Grundnes, J.; Christian, S. D. *J. Am. Chem. Soc.* **1968**, *90*, 2239.
(6) Grundnes, J.; Christian, S. D.; Cheam, V.; Farnham, S. B. *J. Am. Chem. Soc.* **1971**, *93*, 20.
(7) Van Der Helm, D.; Childs, J. D.; Christian, S. D. *Chem. Commun.* **1969**, 887.
(8) Pauling, L. *The Nature of the Chemical Bond*, 3rd ed.; Cornell University Press: Ithaca, NY, 1960; Chapter 7.
(9) Sass, C. S.; Ault, B. S. *J. Phys. Chem.* **1984**, *88*, 432.

0002-7863/91/1513-4732$02.50/0

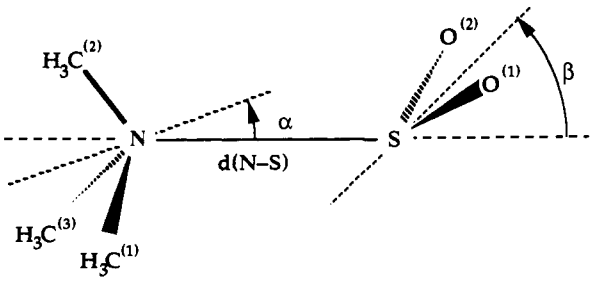

Figure 1. Definition of parameters and atom labels. Angle α is formed by the C_3 axis of trimethylamine and d(N–S); angle β is formed by the C_2 axis of SO_2 and d(N–S).

cm^{-1}. On the other hand, the bending mode shifted to higher frequency by about 33 cm^{-1}. This was explained as due to a steric interaction with the methyl group which staggers the SO_2 bonds. There was no indication of band shifts for the base subunit for any of the complexes.

The experimental data for this complex have prompted several ab initio investigations of its electronic structure which are summarized in Table I. The first calculation with a minimal basis set[10] underestimated the interaction energy and gave an N–S distance of 2.86 Å, while more extensive basis sets gave distances of 2.36 Å[11] and 2.13 Å.[12] In a study by Douglas and Kollman,[11] the binding energies of the methyl-substituted amine complexes with SO_2 were decomposed into electrostatic, polarization, charge-transfer, and exchange-repulsion components using the Morokuma decomposition method.[14] It is interesting that the total binding energies of these complexes (−11.7, −13.9, −14.5, −15.0 kcal/mol) arise from a near cancellation of two large terms (electrostatic and exchange repulsion), while the charge-transfer component of −10.2 to −14.1 kcal/mol reflects the binding energies and the stability trend. The observation that the electrostatic component is the dominant stabilization term, while polarization and charge-transfer terms cannot be neglected in order to reflect stability trends, has been explored more fully and expanded with a model equation for the analysis of noncovalent intermolecular interactions.[15] The photoelectron (PE) spectrum of the $TMA{\cdot}SO_2$ complex has also been reported[13] and shows features between 9.5 and 12.0 eV ascribable to the complex. In combination with MO calculations, it was shown that the observed stabilization of the lone-pair ionization energy of the base upon complexation was proportional to the calculated binding energies and the charge transfer to the sulfur for a series of complexes.

We became interested in studying the rotational spectrum of this complex some years ago but found that the amount of $TMA{\cdot}SO_2$ present in the equilibrium vapor at 250–300 K in a conventional spectrometer, while perhaps detectable, was too small to make ready progress. Expansion through a supersonic nozzle is an excellent method for enhancing the concentration of weakly bound complexes. Coupling this technique to a Fourier transform microwave (FTMW) spectrometer[16] has led to detection of the complexes of SO_2 with TMA,[17] benzene,[18] pyridine,[18] and ethylene.[19] The results of a preliminary study of the $TMA{\cdot}SO_2$ complex are listed in Table I. With data from the normal and ^{34}S isotopic species, the N–S distance was estimated to be between 2.25 and 2.29 Å, which is quite different from the crystal structure. The striking contrast in these values and the absence of much other experimental data to compare the structures of a charge-transfer complex in the gas and crystal phase motivated us to explore this system more fully. We were particularly interested to learn if small changes in the structures of the TMA and SO_2 occur upon complexation. This has led to measurement of the rotational spectra of several isotopic species of $TMA{\cdot}SO_2$ with substitution occurring at all of the heavy atom positions and reinvestigation of the crystal structure at a lower temperature (−70 °C). This paper reports these structural findings and other quantities such as the dipole moment and nitrogen nuclear quadrupole coupling constants obtained from the rotational spectrum. The structural differences between the gas and solid phase will be discussed as well as theoretical models of the complex.

Experimental Section

Materials. The $TMA{\cdot}SO_2$ complex was synthesized by mixing equimolar amounts of TMA (Aldrich) and SO_2 (Matheson) in a vacuum line.[2] The white solid was loaded in a small chamber just upstream from the nozzle tip of a pulsed gas valve. As the material is hygroscopic, a glove box was used to transfer the sample. About 1 to 2 atm of argon was passed through the nozzle chamber which was heated to 50–125 °C to obtain a sufficient pressure of nearly completely dissociated $TMA{\cdot}SO_2$. The higher temperatures were necessary toward the end of a sample run (2–4 days of work) since the sample converted to a viscous liquid after use, probably owing to adventitious water in the system.

The $(CH_3)_3{}^{15}N$ sample was obtained by freeing the amine from the TMA·HCl salt (98% ^{15}N, MSD Isotopes) with sodium hydroxide. Free $(CH_3)_3{}^{15}N$ was passed through a barium oxide column to eliminate the water. Enriched $S^{18}O_2$ (99% ^{18}O, Alfa Organic) was used directly to prepare $TMA{\cdot}S^{18}O_2$. The $SO^{18}O$ sample was obtained by first mixing equimolar amounts of SO_2 and $S^{18}O_2$ in a glass bulb where they quickly equilibrated. The spectra of the ^{13}C and ^{34}S isotopic species were observed in their natural abundancies, which are 1.1 and 4%, respectively.

Spectrometer. The FTMW spectrometer[16] operated in the region of 6.0 to 18 GHz. Our system has been described previously.[20] A modified Bosch fuel injector pulsed nozzle (BOS 0280-150-045) was used with a repetition rate of about 16 Hz. The nozzle orifice was 1.0 mm and the backing pressure of Ar was 1 to 2 atm. Timing of the gas and microwave pulses was coordinated to minimize Doppler splitting of the transitions. Typical line widths of ~20 kHz (fwhm) were observed except for some transitions where hyperfine splittings appeared to complicate and broaden the line shape. Center frequencies were usually reproducible to ±1 kHz and accuracies are estimated to be ±2 kHz.

Spectra. The transitions were characterized by *a*- and *c*-type selection rules and hyperfine splittings due to the ^{14}N nuclear electric quadrupole moment. The hyperfine splittings were helpful in assigning transitions; for example, the similarity in splitting patterns for the *a*-dipole $K = 1$ and $K = 2$ doublets was a useful signature. The observed transitions and hyperfine components are listed in Table II for the normal isotopic species. The splittings were fit to determine the nitrogen quadrupole coupling constants and the unsplit transition frequency. The unsplit centers were fit using a Watson S-reduced Hamiltonia (I^r representation) to obtain the rotational and centrifugal distortion constants. The derived spectroscopic constants are summarized in Table III. A similar procedure was used to assign the transitions from the $(CH_3)_3N{\cdot}{}^{34}SO_2$, $(CH_3)_3{}^{15}N{\cdot}SO_2$, $(CH_3)_3N{\cdot}SO^{18}O$, $(CH_3)_3N{\cdot}S^{18}O_2$, and two different $^{13}CH_3(CH_3)_2N{\cdot}SO_2$ species labeled sym and asy for substitution in and out of the symmetry plane. The rotational and distortion constants are listed in Table III. The observed hyperfine components and unsplit frequencies for the isotopic species are available in Tables S1–S6 as supplementary material (see paragraph at end of paper regarding supplementary material). Internal rotation splittings are quenched in free TMA and none were observed in the complex.

Dipole Moment. To determine the dipole moment, dc voltages of up to ±8 kV were applied with opposite polarities to two steel mesh parallel plates 30 cm apart straddling the microwave cavity.[20a] At each voltage, the Stark-shifted transitions of the complex and of OCS ($J = 0$–1)[21] were measured sequentially. In order to select transitions for which second-order perturbation theory was adequate, exact Stark effect calculations (i.e., diagonalization of the Stark perturbed energy matrices) were ex-

(10) Lucchese, R. R.; Haber, K.; Schaefer, H. F., III *J. Am. Chem. Soc.* **1976**, *98*, 7617.
(11) Douglas, J. E.; Kollman, P. A. *J. Am. Chem. Soc.* **1978**, *100*, 5226.
(12) Sakaki, S.; Sata, H.; Imai, Y.; Morokuma, K.; Onkubo, K. *Inorg. Chem.* **1985**, *24*, 4538.
(13) Pradeep, T.; Sreekanth, C. S.; Hegde, M. S.; Rao, C. N. R. *J. Am. Chem. Soc.* **1989**, *111*, 5058.
(14) Morokuma, K. *Acc. Chem. Res.* **1977**, *10*, 294.
(15) (a) Kollman, P. A. *Acc. Chem. Res.* **1977**, *10*, 365. (b) Kollman, P. A. *J. Am. Chem. Soc.* **1977**, *99*, 4875. (c) Douglas, J. E.; Kollman, P. A. *J. Am. Chem. Soc.* **1980**, *102*, 4293. (d) Kollman, P. A. *J. Am. Chem. Soc.* **1978**, *100*, 2974.
(16) Balle, T. J.; Flygare, W. H. *Rev. Sci. Instrum.* **1981**, *52*, 33.
(17) LaBarge, M. S.; Matos, J.; Hillig, K. W., II; Kuczkowski, R. L. *J. Am. Chem. Soc.* **1987**, *109*, 7222.
(18) LaBarge, M. S.; Oh, J. J.; Hillig, K. W., II; Kuczkowski, R. L. *Chem. Phys. Lett.* **1989**, *159*, 559.
(19) LaBarge, M. S.; Hillig, K. W., II; Kuczkowski, R. L. *Angew. Chem., Int. Ed. Engl.* **1988**, *10*, 1356.
(20) (a) Bohn, R. K.; Hillig, K. W., II; Kuczkowski, R. L. *J. Phys. Chem.* **1989**, *93*, 3456. (b) Hillig, K. W., II; Matos, J.; Scioly, A.; Kuczkowski, R. L. *Chem. Phys. Lett.* **1987**, *133*, 359.
(21) Muenter, J. S. *J. Chem. Phys.* **1968**, *48*, 4544.

Table II. Observed Transition Frequencies for $(CH_3)_3N{\cdot}SO_2$

transition	F′	F	ν_{obs}[a]	$\Delta\nu$[b]	transition	F′	F	ν_{obs}[a]	$\Delta\nu$[b]
$2_{11}-1_{01}$			8340.701	−1	$4_{04}-3_{03}$			12684.643	1
	2	1	8341.090	0		3	2	12684.556	1
	3	2	8340.665	0		4	3	12684.662	−3
	2	2	8340.034	0		5	4	12684.662	1
						3	3	12686.084	2
$2_{21}-1_{11}$			11259.620	2		4	4	12683.533	−1
	1	0	11259.719	−2					
	2	1	11260.009	0	$4_{14}-3_{13}$			12421.312	−2
	3	2	11259.468	2		3	2	12421.317	−3
						4	3	12421.230	1
$2_{20}-1_{10}$			11065.290	1		5	4	12421.363	2
	1	0	11065.201	0		4	4	12420.423	1
	2	1	11065.765	−2		3	3	12422.408	−1
	3	2	11065.122	2					
					$4_{13}-3_{12}$			13279.471	0
$3_{12}-2_{02}$			11897.225	1		3	2	13279.469	1
	2	1	11896.924	1		4	3	13279.388	−3
	3	2	11897.382	−3		5	4	13279.523	1
	4	3	11897.214	2					
					$4_{23}-3_{22}$			12878.014	0
$3_{22}-2_{12}$			14700.199	−2		3	2	12878.264	1
	2	1	14699.806	−4		4	3	12877.664	−1
	3	2	14700.588	0		5	4	12878.141	0
	4	3	14700.089	2		3	3	12878.264	1
	2	2	14700.588	0		4	4	12877.664	−1
	3	3	14700.089	2					
					$4_{22}-3_{21}$			13088.759	1
$3_{21}-2_{11}$			14160.446	−1		3	2	13089.020	0
	2	1	14159.980	−1		4	3	13088.389	1
	3	2	14160.904	−1		5	4	13088.894	0
	4	3	14160.319	2					
					$4_{32}-3_{31}$			12936.240	−1
						3	2	12936.901	−2
$3_{03}-2_{02}$			9583.656	0		4	3	12935.442	−1
	2	1	9583.468	0		5	4	12936.500	3
	3	2	9583.671	−4					
	4	3	9583.693	2	$4_{31}-3_{30}$			12944.910	1
	2	2	9585.201	0		3	2	12945.575	0
	3	3	9582.562	2		4	3	12944.112	1
						5	4	12945.167	−1
$3_{13}-2_{12}$			9333.260	0					
	2	1	9333.352	−3	$5_{15}-4_{14}$			15493.493	−3
	3	2	9333.044	0		5	4	15493.453	−2
	4	3	9333.352	2		6	5	15493.523	2
	3	3	9332.544	1					
					$5_{14}-4_{13}$			16547.101	−3
$3_{12}-2_{11}$			9981.942	1		5	4	16547.068	0
	2	1	9982.011	−5					
	3	2	9981.727	0	$5_{23}-4_{22}$			16458.884	2
	4	3	9982.041	4		5	4	16458.690	−3
	2	2	9982.999	1		6	5	16458.963	−3
	3	3	9981.096	0		4	3	16458.997	5
$3_{22}-2_{21}$			9671.676	1	$5_{24}-4_{23}$			16069.485	1
	2	1	9672.557	1		5	4	16069.313	−1
	3	2	9670.797	1		6	5	16069.554	−4
	4	3	9671.926	−1		4	3	16069.588	5
	2	2	9670.797	1					
	3	3	9671.926	−1	$5_{33}-4_{32}$			16182.080	0
						5	4	16181.680	0
$3_{21}-2_{20}$			9759.684	0		6	5	16182.227	0
	2	1	9760.577	1		4	3	16182.360	0
	3	2	9758.786	0					
	4	3	9759.942	−1	$5_{32}-4_{31}$			16211.963	0
						5	4	16211.558	−1
$5_{05}-4_{04}$			15729.174	3		6	5	16212.111	−1
	4	3	15729.121	0		4	3	16212.248	2

[a] Observed frequency (ν_{obs}) in MHz. The first frequency listed for each transition is ν_0, the center frequency in the absence of hyperfine splitting. [b] Observed − calculated frequency in kHz using A, B, C, D_J, etc., in Table III to calculate the center frequency and the quadrupole coupling constants for the hyperfine components.

amined to eliminate transitions which did not vary strictly with the square of the electric field (E^2).

The second-order Stark effects ($\Delta\nu/E^2$) for 10 M_J components from five transitions of the $(CH_3)_3{}^{15}N{\cdot}SO_2$ species were determined. The ^{15}N species was chosen since it is free of nitrogen hyperfine splittings. A least-squares fit of $\Delta\nu/E^2$ using the calculated second-order coefficients gave the dipole components μ_a = 4.676 (5), μ_c = 1.081 (4), and μ_{total} = 4.800 (5) D. The value of μ_b was held to zero in the fitting due to the *ac*-symmetry plane in the complex (see the Structure section). When $\mu_b{}^2$ was not fixed to zero, the least-squares fit determined a value for it very nearly equal to zero [$\mu_b{}^2$ = 0.003 (3) D^2]. The experimental values of $\Delta\nu/E^2$ are available in Table S7, supplementary material. The agreement between the experimental and calculated values of $\Delta\nu/E^2$ was good; the root-mean-square deviation was 0.71%.

Crystallographic Study. Owing to the hygroscopic property of the solid, many attempts to grow a single crystal and transfer it to a capillary tube were made. The most successful procedure employed a vacuum line. After being pumped on the vacuum line and a reaction finger for about 2 days, the complex was synthesized in the finger by condensing TMA and SO_2 in it and warming. The reactants had both been purified by passage through dry ice–acetone traps. An X-ray capillary tube was connected to an inlet on the vacuum line close to the reaction finger, and a small amount of the complex was transferred to the capillary by cooling it below room temperature. The capillary was sealed and the complex was repeatedly sublimed by keeping one end of the capillary slightly below room temperature. Prospective crystals for X-ray analysis were stored in a freezer at about −30 °C.

Intensity data at −70 °C were recorded on a Siemens R3m/v diffractometer equipped with an LT-2 low-temperature device using Mo Kα radiation (λ = 0.71073 Å) with a $\theta/2\theta$ scan method. Two standard reflections were monitored every 48 reflections and found to be constant. Background counts were measured for a total of one-half the scan time. The intensities were corrected for Lorentz and polarization effects but not for absorption because of the small size of the crystal. Reflections with $|F_o| < 4\sigma(F)$ were omitted. The refined cell constants from 13 reflections ($20.6° < 2\theta < 30.5°$) and additional relevant crystal data are given in Table IV.

The structure was solved by the Patterson method and refined by the full matrix least-squares method. All calculations were performed on a VAXstation 3500 using the Siemens SHELXTL Plus program package. Atomic scattering factors and anomalous dispersion terms were taken from ref 22 provided as part of the Siemens software. The agreement factors were defined by $R = \Sigma((|F_o| - |F_c|)/\Sigma|F_o|)$, $R_w = [\Sigma(|F_o| - |F_c|)^2/\Sigma_w|F_o|^2]^{1/2}$, $w = [\sigma^2(F_o) + 0.001070(F_o)^2]$. Hydrogen atoms were located on a difference Fourier map and were allowed to refine with isotropic thermal parameters. The heavy atom fractional coordinates are shown in Table V. Thermal parameters, hydrogen parameters (Table S9 and S10), and structure factors (Table S11) are available as supplementary material.

Results and Discussions

Structure. The gas-phase structural information is contained in the principal moments of inertia, I_a, I_b, I_c, which are derivable from the spectroscopic constants, A, B, C, i.e., $I_a = h/(8\pi^2A) = \Sigma_i m_i(b_i^2 + c_i^2)$, etc.[23] The second moments $P_{bb} = (I_a + I_c - I_b)/2 = \Sigma_i m_i b_i^2$ for the normal, ^{34}S, ^{15}N, and one of the ^{13}C isotopic species ($^{13}C^{sym}$) are 100.639, 100.639, 100.634, and 100.635 amu Å^2, respectively. Although these P_{bb} values of the complexes are about 1 amu Å^2 larger than the sum (99.614 amu Å^2) calculated from the structures of free TMA[24] and SO_2,[25] the good agreement between the isotopes is clearly consistent with the expected C_s symmetry for the complex and indicates that the nitrogen, sulfur, and one carbon atom lie in the *ac* symmetry plane. Since the μ_b component of the dipole moment was also consistent with C_s symmetry, we assumed an *ac* symmetry plane throughout the analysis of the structure of this complex in the gas phase.

The differences between the calculated and observed P_{bb} can arise from two sources: (a) a change in structural parameters of TMA and/or SO_2 upon complexation, and (b) large amplitude vibrational motions in the complex. The actual differences are small, and similar values are observed for other weakly bound complexes where they are believed to arise principally from vibrational effects. It is difficult to estimate these effects on the moments of inertia and corrections were not attempted. We instead used least-squares fitting of all the moments of inertia both assuming no changes in the TMA and SO_2 parameters and upon

(22) *International Tables for X-ray Crystallography*; Kynoch, Press: Birmingham, England, 1974; Vol. IV.
(23) The conversion factor $h/(8\pi^2)$ = 505 379.05 amu Å^2 MHz was used.
(24) (a) Wollrab, J. E.; Laurie, V. W. *J. Chem. Phys.* **1969**, *51*, 1580. (b) Lide, D. R.; Mann, D. E. *J. Chem. Phys.* **1958**, *28*, 572.
(25) (a) Harmony, M. D.; Laurie, V. W.; Kuczkowski, R. L.; Schwendeman, R. H.; Ramsay, D. A.; Lovas, F. J.; Lafferty, W. J.; Maki, A. G. *J. Phys. Chem. Ref. Data* **1979**, *8*, 619. (b) Patel, D.; Margolese, D.; Dyke, T. R. *J. Chem. Phys.* **1979**, *70*, 2740.

Table III. Spectroscopic Constants for the Isotopic Species of $(CH_3)_3N{\cdot}SO_2$

	normal	^{34}S	^{15}N	^{18}O	$^{18}O_2$	^{13}C(asy)[c]	^{13}C(sym)[c]
no. of lines[a]	25 (85)	13 (33)	27	23 (56)	10 (30)	13 (37)	8 (24)
A/MHz	3179.7743 (20)	3172.6879 (20)	3179.9485 (3)	3120.1852 (3)	3057.8462 (114)	3144.7924 (21)	3137.942 (92)
B/MHz	1720.3180 (4)	1703.2487 (7)	1713.7066 (2)	1695.6093 (3)	1673.2338 (5)	1702.7560 (7)	1700.2360 (31)
C/MHz	1503.5985 (4)	1492.1069 (4)	1498.5495 (2)	1472.6997 (3)	1443.2285 (5)	1485.1878 (5)	1497.6105 (14)
D_J/kHz	0.835 (4)	0.808 (8)	0.817 (3)	0.792 (3)	0.778 (6)	0.804 (7)	0.824 (20)
D_{JK}/kHz	−0.786 (15)	−0.755 (54)	−0.738 (13)	−0.751 (13)	−0.764 (61)	−0.726 (50)	−0.614 (296)
D_K/kHz	0.803 (408)	0.803[d]	0.803[d]	0.803[d]	0.803[d]	0.803[d]	0.803[d]
d_1/kHz	−0.102 (4)	−0.094 (8)	−0.092 (3)	−0.098 (3)	−0.091 (9)	−0.103 (10)	−0.093 (38)
d_2/kHz	0.030 (2)	0.020 (5)	0.031 (2)	0.033 (2)	0.028 (4)	0.028 (4)	−0.013 (31)
$\Delta\nu_{rms}$/kHz[b]	1.6	1.4	1.5	1.4	0.9	1.3	1.5
χ_{aa}/MHz	−3.520 (2)	−3.534 (5)		−3.504 (2)	−3.496 (5)	−3.499 (6)	−3.550 (16)
χ_{bb}/MHz	1.963 (2)	1.951 (6)		1.958 (2)	1.940 (20)	1.947 (9)	1.970 (15)

[a] Number in parentheses is the number of measured quadrupole components. [b] $\Delta\nu = \nu_{obs} - \nu_{calc}$. [c] ^{13}C(asy) is substitution at C1 or C3 in Figure 1; ^{13}C(sym) is at C2. [d] Fixed to the value for the normal isotope.

Table IV. Summary of Crystal Data for $(CH_3)_3N{\cdot}SO_2$

compound	trimethylamine·SO_2
formula	$C_3H_9NSO_2$
formula weight	139.170 amu
crystal dimensions/mm	0.10 × 0.06 × 0.12
crystal system	monoclinic
space group	$P2_1/n$(#14)
a	5.755 (5) Å
b	10.656 (9) Å
c	10.257 (7) Å
β	104.55 (6)°
density (calc)	1.51 (8) g cm^{-3}
F(000)	265 electrons
octants collected	$+h, +k, \pm l$ (h:0/7; k:0/13; l:−13/13)
volume	608.8 (7) Å^3
Z	4
linear absorption coefficient	4.1 cm^{-1}
temperature	−70°
scan type	$\theta/2\theta$ scan
scan width	0.8° below Kα_1 to 0.8° above Kα_2
scan speed	2–5 deg/min, variable
2θ scan range	5–50°
total no. of data collected	1317
no. of unique reflections	1057, R_{int} = 0.0474
reflections with $\lvert F_o\rvert > 4\sigma(\lvert F_o\rvert)$	711
no. of parameters refined	101
R	0.0672
R_w	0.0765
GOF	1.62
residual electron density	+0.458/−0.581 e/Å^3
forms of weighting	$\{\sigma^2(F_o)^2 + 0.001\,070(F_o)^2\}^{-1}$

Table V. Fractional Coordinates for $(CH_3)_3N{\cdot}SO_2$ from X-ray Analysis

atom	x	y	z	U(eq)[a]
S	0.0488 (3)	0.2524 (2)	0.6524 (2)	0.0302 (5)
O(1)	−0.1538 (9)	0.1690 (4)	0.6139 (4)	0.043 (2)
N	−0.1049 (8)	0.3932 (4)	0.7377 (4)	0.018 (1)
C(1)	−0.191 (1)	0.3401 (7)	0.8490 (7)	0.032 (2)
C(2)	−0.307 (1)	0.4439 (6)	0.6316 (6)	0.028 (2)
C(3)	0.083 (1)	0.4884 (7)	0.7858 (7)	0.033 (2)

[a] U(eq) is defined as one-third the trace of the orthogonalized U_{ij} matrix.

relaxing that condition as a means of obtaining insight into the possibility of changes in the structural parameters upon complexation. The two fits are reported in Table VI. In one fit (I), all the monomer structural parameters were fixed, and the center of mass distance (R_{cm}) and the tilt angles of the symmetry axes of TMA and SO_2 with respect to R_{cm} were fitted to the observed moments of inertia for the seven isotopes. In the other fit (II), all the heavy atom coordinates were varied. In these two calculations, the methyl groups were assumed to have local C_3 symmetry with the average values found for free TMA. The derived parameters were not very sensitive to the methyl group parameters; when the C–H distance was changed by ±0.01 Å, the other

Table VI. Structural Parameters (Å, deg) for $(CH_3)_3N{\cdot}SO_2$

	I[a]	II[c]	Kr[d]	X-ray
R(N–S)	2.328	2.285	2.260 (30)	2.046 (4)
S–O1[e]	1.431[b]	1.435	1.444 (10)	1.441 (5)
S–O2	1.431[b]	1.435	1.444 (10)	1.433 (5)
N–C1	1.451[b]	1.468	1.461 (15)	1.481 (7)
N–C2	1.451[b]	1.455	1.468 (10)	1.468 (7)
N–C3	1.451[b]	1.468	1.461 (15)	1.474 (8)
S–N–C2	110.5	104.3	104.3 (20)	107.3 (3)
S–N–C1	106.7	107.6	107.9 (20)	108.5 (4)
S–N–C3	106.7	107.6	107.9 (20)	106.8 (3)
O–S–O	119.5[b]	117.9	116.9 (20)	113.7 (3)
O1–S–N	91.1	95.6	95.9 (20)	99.4 (2)
O2–S–N	91.1	95.6	95.9 (20)	98.4 (2)
C2–N–C1	110.9[b]	112.6	111.8 (10)	110.8 (5)
C2–N–C3	110.9[b]	112.6	111.8 (10)	111.7 (4)
C1–N–C3	110.9[b]	111.7	112.6 (10)	111.5 (4)
α[f]	2.5	0.8	0.8 (10)	∼0
β[f]	87.8	79.0	78.5 (20)	73.6 (2)

[a] Least-squares fit of all isotopic data holding TMA and SO_2 geometries fixed. [b] Values fixed from free TMA[24] and SO_2.[25] Also, d(CH) = 1.10 Å, ∠HCN = 110.5°. [c] Least-squares fit allowing TMA and SO_2 parameters to vary except for d(CH)[b] and ∠HCN.[b] [d] Gas-phase structure recommended by authors. Calculated from Kraitchman substitution coordinates in Table VII. Data from double ^{18}O data gave the same value of 1.444 Å, 116.9°, and 95.9° for d(SO), ∠OSO and ∠OSN, respectively. Uncertainty estimates in parentheses. [e] See Figure 1 for atom numbering. [f] See Figure 1 for definition. α is calculated assuming symmetric methyl groups.

Table VII. Heavy Atom Coordinates for $(CH_3)_3N{\cdot}SO_2$ (Å) from Isotopic Data

	|a|		|b|		|c|	
	Kr[a]	II[a]	Kr	II	Kr	II
S	1.147	1.162	0.0	0.0	0.428	0.420
O	1.434[b]	1.439	1.230[b]	1.230	0.271[b]	0.266
N	1.072	1.082	0.0	0.0	0.0	0.014
C(sym)	1.157	1.166	0.0	0.0	1.466	1.467
C(asy)	1.641	1.649	1.216	1.215	0.577	0.584

[a] Coordinate from Kraitchman (Kr) substitution method or least-squares fitting of moments of inertia (II). [b] Same value was obtained from both single and double ^{18}O substitution.

parameters changed less than the differences between the two fits. The overall quality of the fits was excellent with ΔI_{rms} = 0.021 amu Å^2; the detailed values for $\Delta I = I_{obs} - I_{calc}$ are available as supplementary data (Table S8).

In addition to the least-squares method, Kraitchman[26] has given a convenient method for calculation of the position of an atom in a molecule which utilizes the changes in moments of inertia resulting from an isotopic substitution. Using all the heavy atom substitution data available, the heavy atom principal axis coordinates from the Kraitchman method were calculated and are

(26) Kraitchman, J. *Am. J. Phys.* **1953**, *21*, 17.

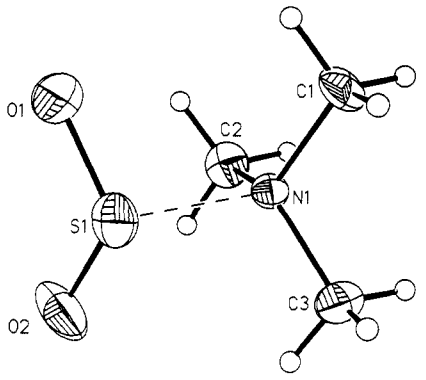

Figure 2. ORTEP drawings of the crystal structure of $(CH_3)_3N{\cdot}SO_2$ (50% probability ellipsoids).

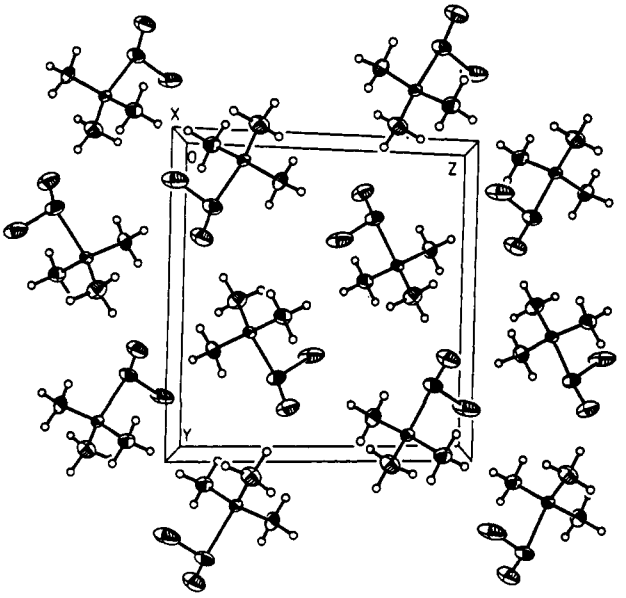

Figure 3. Packing diagram for the $(CH_3)_3N{\cdot}SO_2$ crystal.

shown in Table VII. The structural parameters from this method are shown in Table VI as the "Kr" values.

The crystal structure, obtained with an R value of 0.067, is also given in Table VI (X-ray). The structure is in good agreement with the earlier X-ray study at room temperature[7] considering that R was 0.14 in that work. The C_3 axis of the TMA points to sulfur, and the angle between the SO_2 plane and the N–S distance is calculated to be 73.6°. Illustrations of the crystal structure and packing are shown in Figures 2 and 3.

The differences between the three derived gas-phase structures are small except for d(N–S) and the tilt angles (α, β) associated with the relative orientations of TMA and SO_2. These differences are not surprising; in fit I, these three parameters must take up all the effects from neglect of vibrational averaging and any small changes in TMA and SO_2. On the other hand, relaxing the constraints (II) does not lead to changes in the other heavy atom parameters which are large enough to clearly indicate changes in the TMA or SO_2 upon complexation. There is an indication that d(NC) and d(SO) have lengthened while ∠OSO has decreased; however, the changes are small enough to be artifacts from the neglect of vibrational effects. We conclude that in the gas-phase complex any changes upon complexation are small (≤0.015 Å for bond distances, 1–2° for bond angles) and not unambiguously established. Since there is expected to be some cancellation of vibrational effects for the Kraitchman structure, we recommend those values as the preferred set. The differences between the structures of I and II give operational error estimates which probably encompass model errors due to neglect of vibrational effects for most of the parameters. The error estimates chosen for the Kr structures in Table VII were guided by these differences.

Examination of the TMA and SO_2 parameters in the crystal suggests a small, but possibly insignificant lengthening in d(S–O), similar to the gas-phase complex. The larger increase in d(C–N) and the decrease in ∠OSO seem to more clearly signify small changes in the TMA and SO_2 upon complexation. There also appears to be a decrease in the SO_2 tilt angle (β) of several degrees from the gas-phase complex and, of course, the decrease in d(N–S) of about 0.2 Å in the crystal is striking. This latter change is not an artifact of vibrational effects which have been neglected. An estimate of the mean-squared vibrational amplitude for the N–S distance due to the stretching vibration between TMA and SO_2 gave 0.064 Å[27] for the gas-phase complex. In the solid state, the thermal parameters for nitrogen and sulfur are 0.02 and 0.03 Å. Thus, the difference in d(N–S) is too large to arise from vibrational motion. In summary, the crystal structure shows a number of small and large changes compared to the gas-phase complex and free TMA and SO_2. It is interesting that a systematic trend is found for many of the changes in going from free TMA and SO_2, via the gas-phase complex, to the crystal. This would correlate with a stronger interaction between TMA and SO_2 in the crystal as indicated by the shorter N–S distance, with a commensurate tendency for electronic reorganization in the TMA and SO_2. However, since the small changes are marginal effects whose magnitude may not be completely unambiguous, our discussion will focus on the two clearly significant changes involving d(N–S) and ∠OSO.

The obvious inference from both of these changes is that they signify a stronger interaction between TMA and SO_2 in the crystal compared to the gas-phase complex. The correlation between a shorter N–S distance in the crystal and a stronger interaction needs little comment. The rationale associated with ∠OSO is based on noting a similar decrease for this parameter in SO_2^- to about 114°[28a] and correlating this change with an increase in the charge transfer from nitrogen to the SO_2. There is also evidence for a similar decrease for this angle in numerous η^1-pyramidal SO_2 complexes with transition metals.[28b] The sensitivity of the interaction between SO_2 and TMA to environment is also reflected in the large blue shift for the charge-transfer band in a polar solvent and the different dissociation energies in the gas phase and in heptane, as noted in the Introduction. The IR results (matrix)[9] also show a sensitivity in the SO_2 stretching and bending frequencies but apparently not in the TMA frequencies. The increase in the SO_2 bending frequency correlates nicely with the decrease in the OSO angle. The decrease in the SO stretch and apparent absence of effect on CN frequencies compare with perhaps a slight increase in d(SO) and an increase in d(CN).

Two mechanisms can be envisioned to rationalize the change in d(N–S) from gas to crystal. They originate in crystal and packing interactions but differ in focus. The first mechanism identifies close contacts between adjacent complexes as a sign of special interactions in the solid. Visual inspection of the unit cell in Figure 3 suggests that the oxygen atoms appear to be oriented favorably to interact with hydrogens on neighboring complexes. Indeed several O···H contacts are in the range of 2.55–2.85 Å which is relatively short given the van der Waals radii of O and H of 1.70 Å and 1.20 Å.[29] No doubt these intermolecular interactions contribute some stabilization to the lattice although they are not so readily connected to an increased intramolecular interaction between TMA and SO_2 and a decrease in d(N–S). The second mechanism is based on correlating the decrease in d(N–S) with an increased dipole moment for the complex, which thereby increases the lattice stabilization. As a simple test of this hypothesis we calculated the binding energy and dipole moment of the complex as a function of N–S distance. Using GAUSSIAN86,[30]

(27) This estimate was obtained from a harmonic oscillator model using the force constant obtained from the pseudo-diatomic approximation. See the final section.

(28) (a) Hirao, K. *J. Chem. Phys.* **1985**, *83*, 1433. (b) Ryan, R. R.; Kubas, G. J.; Moody, D. C.; Eller, P. G. *Struct. Bonding (Berlin)* **1981**, *46*, 47.

(29) Bondi, A. *J. Phys. Chem.* **1964**, *68*, 441. The four shortest O···H contacts are 2.55, 2.72, 2.73, and 2.85 Å (see Figure 3).

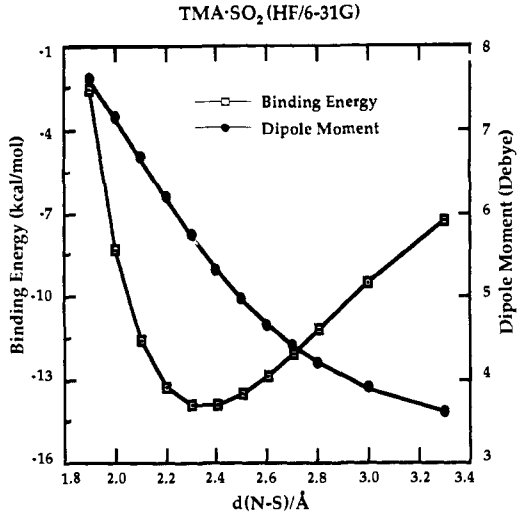

Figure 4. Binding energy and dipole moment versus N–S distance calculated by GAUSSIAN86 (HF/6-31G; β optimized at each point, β = 80.2° at minimum).

the N–S distance was varied between 1.9 to 3.3 Å while the tilt angle of the SO_2 plane was also optimized. In this calculation (HF/6-31G), the C_3 symmetry of TMA was maintained and the C_3 axis was pointed directly to the sulfur atom. The minimum in energy is located at d(N–S) = 2.35 Å and β = 80.7° with μ = 5.2 D, in fair agreement with experiment. The energy change with N–S distance is rather flat near the minimum (see Figure 4) while μ increases and β decreases systematically as d(N–S) is decreased. The detailed variation in d(N–S), β, dipole moment, and the binding energy is available in Table S12. It is seen that shortening d(N–S) by 0.2 Å from the calculated minimum will destabilize the complex by about 2 kcal/mol while μ increases by about 1.1 D. This dipole moment change presumably arises from increased overlap of the atomic orbitals on N and S and greater charge transfer to the sulfur.

Placing the gas-phase dipole moment of 4.8 D at the middle of the N–S bond axis and using the crystal structure coordinates and symmetry for the complex, a dipole–dipole interaction energy contribution to the lattice energy of 5.9 kcal/mol can be calculated which is well below the experimental sublimation energy of 17.1 kcal/mol. An increase in the dipole moment by 1.1 D will raise the lattice energy by about 3 kcal/mol, neglecting intramolecular repulsion effects. This simple approach suggests that an increase in the dipole moment in the solid is plausible and can provide for some increase in the lattice stabilization, although the agreement is only qualitatively correct. Of course, the model is simplistic both at the level of the MO calculation and in the crude approximation used to estimate the lattice energy.

While the mechanisms discussed above are speculative, the sensitivity of the structure to the crystal environment is clear and must ultimately be associated with increased interactions arising in the solid state. The question arises whether $TMA{\cdot}SO_2$ is unusual or whether the structure of other charge-transfer complexes are similarly sensitive to environment. Unfortunately, there is a paucity of data to permit an empirical answer. While there is extensive X-ray data on donor–acceptor complexes,[31] there is a dearth of gas-phase structural results. One other example which we are aware of involves the complexes between TMA and halogens. X-ray studies indicate that the halogen is attached colinearly with the symmetry axis of the TMA in $TMA{\cdot}I_2$[32a] and TMA·ICl.[32b] Theory also predicts C_{3v} symmetry for the simpler systems, $NH_3{\cdot}Cl_2$ and $NH_3{\cdot}ClF$.[33] However, a recent gas-phase diffraction study of $TMA{\cdot}Br_2$ indicated that the Br_2 was bent away from the symmetry axis; sizable changes in the TMA parameters were also reported.[34] For somewhat stronger complexes ($\Delta H_{diss} \geq 20$ kcal/mol) with large dipole moments, such as in $Me_3N{\cdot}BF_3$[35] and $Me_3P{\cdot}BH_3$,[36] complementary gas-phase and crystal data indicate that the central dative bond distances usually agree to about ±0.03 Å. It is also interesting that the distance of 4.4475 (2) Å between the centers-of-mass of the monomers in the linear hydrogen-bonded HCN dimer[37] shortens to 4.34 (2) Å between adjoining HCNs in the solid.[38] The solid consists of parallel linear chains of HCN in the high-temperature form.

As noted in the Introduction, four theoretical calculations (HF–SCF) of $TMA{\cdot}SO_2$ have been reported. The later calculations with the more sophiscated basis sets reproduce d(N–S) to about 0.1 Å, the two tilt angles α and β to about $1 \sim 5°$, and ΔE_{diss} to about 5 kcal/mol. This agreement is gratifying since it indicates that, for complexes of this type, the neglect of correlation effects does not seriously compromise the gross structural and energetic conclusions, unless high accuracy is desired (as noted previously[12]). The Morokuma energy decomposition scheme argues that the binding energy is distributed among electrostatic, charge-transfer and polarization effects in the ratio of 6:3:1[11] and that the directionality of the amine·SO_2 interaction is dominated by the electrostatic energy.[15a] Extending this concept to a simple charge distribution model for amine and SO_2 leads to a chemically appealing and simple interpretation for the gross geometry, viz., the interaction of the nitrogen end of TMA where a large negative potential occurs with the sulfur end of SO_2 where a large out-of-plane positive potential resides. Another gas-phase complex with a similar geometry but apparently weaker interaction is $HCN{\cdot}SO_2$; the N–S distance is 2.98 Å and β is 80°.[39]

Dipole Moment and Quadrupole Coupling Constants. Simple interpretations of these two quantities correlate well with a modest charge-transfer component in the complex. The dipole moments of free SO_2 (1.633 D)[25b] and TMA (0.612 D)[24b] would predict a dipole moment of 1.84 D for the complex. The difference between this and the observed value (4.80 D) can be attributed to electronic redistribution composed of polarization and charge-transfer effects. If these are combined into a single charge-transfer term, an upper limit of 0.32 electron is transferred from nitrogen to sulfur. The small amount of charge transfer suggested by this is compatible with the other evidence for an interaction weaker than a normal covalent bond.

In the case of the nitrogen quadrupole coupling constants (Table III), the near equivalence in eQq_{bb} and eQq_{cc} suggests that the C_3 symmetry of the quadrupole tensor in the free TMA is only slightly perturbed upon complexation. If it is assumed that the principal axis of the tensor is likewise little perturbed and lies along the local C_3 axis of TMA in the complex, one predicts a value for eQq_{zz} of −3.760 MHz from the observed value of eQq_{aa} and the value of 12.1° from fit II (Table VI) for the angle between the a inertial axis and the C_3 axis of TMA.

The significant change of the nuclear quadrupole coupling constant along this axis from free TMA (−5.47 MHz)[24] is too large to arise from vibrational averaging effects and reflects the charge-transfer and polarization effects. For example, the change in χ_{bb} would imply an average out-of-plane bending amplitude of 25.7° which is unreasonable. Since the nuclear quadrupole coupling constants depend on $1/\langle r^3 \rangle$ for the electrons around the nucleus, we can estimate the relative population of the nitrogen orbitals in the valence shell. By taking the approach used by

(30) Frisch, M. J.; Binkley, J. S.; Schlegel, H. B.; Raghavachari, K.; Melius, C. F.; Martin, R. L.; Stewart, J. J. P.; Bobrowicz, F. W.; Rohlfing, C. M.; Kahn, L. R.; DeFrees, D. J.; Seeger, R.; Whiteside, R. A.; Fox, D. J.; Fluder, E. M.; Pople, J. A. GAUSSIAN86; Carnegie-Mellon Quantum Chemistry Publishing Unit: Pittsburgh, PA, 1986.
(31) Prout, C. K.; Karnevar, B. *Molecular Complexes*; Foster, R., Ed.; Crane, Russak: New York, NY, 1973; Vol. 1, Chapter 4.
(32) (a) Strømme, K. O. *Acta Chem. Scand.* **1959**, *13*, 268. (b) Hassel, O.; Hope, H. *Acta Chem. Scand.* **1960**, *14*, 391.
(33) Umeyama, H.; Morokuma, K.; Yamabe, S. *J. Am. Chem. Soc.* **1977**, *99*, 330.
(34) Shibata, S.; Iwata, J. *J. Chem. Soc., Perkin Trans. 2* **1985**, 9.
(35) Bryan, P. S.; Kuczkowski, R. L. *Inorg. Chem.* **1972**, *11*, 553.
(36) (a) Cassoux, P.; Kuczkowski, R. L.; Serafini, A. *Inorg. Chem.* **1977**, *16*, 3005. (b) Geller, S.; Hoard, L. J. *Acta Crystallogr.* **1951**, *4*, 399.
(37) (a) Buxton, L. W.; Campbell, E. J.; Flygare, W. H. *Chem. Phys.* **1981**, *56*, 399. (b) Georgiou, K.; Legon, A. C.; Millen, D. J.; Mjöberg, P. J. *Proc. R. Soc. London, Ser. A* **1985**, *399*, 377.
(38) Dulmage, W. J.; Lipscomb, W. N. *Acta Crystallogr.* **1951**, *4*, 330.
(39) Goodwin, E. J.; Legon, A. C. *J. Chem. Phys.* **1986**, *85*, 6828.

Lucken[40] and others,[41,42] an equation can be derived, $eQq/eQq_0 = -3\cos\alpha/(1-\cos\alpha)\{a-b\}$, where a and b are the populations of the nitrogen lone electron pair and the N–C bond population, respectively, and α is the C–N–C angle. Using the experimentally determined angle of 111°, and $eQq_0 = -9.0$ MHz[40] the value of $a-b$ can be calculated for free TMA and the complex. For free TMA it is 0.768. For the complex, using $eQq_{zz} = -3.760$, it is 0.528. These calculations show that the population difference is reduced by about 0.24 electron. Since the C–N bond is not likely to be the major source of the change in the electron density, this implies that the lone-pair electrons of the nitrogen partially transfer to the sulfur atom in the SO_2.

These estimates of charge transfer to sulfur are somewhat higher than from MO calculations[12,13] which give an increase of 0.15 electron at sulfur from the reported Mulliken population analysis. Of course, the dipole and quadrupole analyses neglected any corrections for vibrational averaging effects on the parameters, but the magnitude of these effects are not large enough to warrant detailed consideration given the simplicity of the models used to interpret them.

Centrifugal Distortion Constants. Interpretation of the distortion constants for asymmetric rotors is considerably more complex than for linear or symmetric top molecules. However, for weakly bonded complexes (≤5 kcal/mol), the largest contribution usually arises from the new stretching mode between the two moieties. Commonly the pseudodiatomic approximation which neglects contributions to the distortion constant D_J from all vibrational modes except the stretching mode is used to interpret the distortion constants.[43] Using this approximation and D_J in Table III, the stretching force constant was estimated to be 0.301 mdyn/Å, and the associated vibrational frequency was 129 cm^{-1}. Based on the Lennard-Jones 6-12 (LJ 6-12) potential, the binding energy was calculated to be about 4.5 kcal/mol which is much lower than the experimental value of 9.1 kcal/mol. This difference is partly due to the potential function which is used. It has been observed by Kollman et al. that the intermolecular interaction in many complexes is better approximated by setting the attractive term proportional to the inverse fifth power.[15] If we use this 5–10 potential form, the calculated binding energy of 7.1 kcal/mol agrees somewhat better. It is interesting that if we fit the calculated potential function for the complex in Figure 4 to a Lennard-Jones $n-2n$ form, a value of n of 3.15 (5) is estimated. This also shows that the repulsive wall is very soft and that the LJ 6-12 potential form is inappropriate as a binding model or to estimate the dissociation energy for this strong complex. Of course, the nearly $1/R^3$ dependence of the attractive term is close to a pure dipole–dipole term, also emphasizing the electrostatic interaction found in this complex. This reinforces the conclusion from the ab initio calculation and Morokuma decomposition procedure[15] which pointed out the importance of the electrostatic component in the overall binding energy for TMA-SO_2.

Acknowledgment. The authors acknowledge the help of Professors L. Lohr with ab initio calculations, C. E. Nordman with advice on crystal growing, and R. C. Taylor who supplied programs and advice on the vibrational analyses. They are grateful to the donors of the Petroleum Research Fund, administered by the American Chemical Society, for support of this work. The research was also supported by the National Science Foundation, Washington, DC.

Supplementary Material Available: Tables of hyperfine fitting of observed transition frequencies and centrifugal distortion fitting of the unsplit frequencies, Stark effect data, structure fitting data, thermal parameters, hydrogen atomic parameters, and ab initio binding energies and dipole moments (8 pages); listing of structure factors (4 pages). Ordering information is given on any current masthead page.

(40) Lucken, E. A. C. *Nuclear Quadrupole Coupling Constants*; Academic: New York, 1969.
(41) Gordy, W.; Cook, R. L. *Microwave Molecular Spectra*; 3rd ed.; Wiley: New York, 1984.
(42) Townes, C. H.; Schawlow, A. L. *Microwave Spectroscopy*; MaGraw-Hill: New York, 1955.
(43) Millen, D. J. *Can. J. Chem.* **1985**, *63*, 1477.

Use of Gas-Phase Basicities for the Study of Solution Kinetics: An Unprecedented Extension of Brønsted Correlations

José-Luis M. Abboud,*,† Rafael Notario,† Juan Bertrán,‡ and Robert W. Taft§

Contribution from the Instituto de Química Física "Rocasolano", CSIC, c/ Serrano, 119, E-28006 Madrid, Spain, Departamento de Química Física, Facultad de Ciencias, Universidad Autônoma de Barcelona, E-08193 Bellaterra (Barcelona), Catalonia, Spain, and Department of Chemistry, University of California, Irvine, California 92717. *Received November 16, 1990*

Abstract: Activation free energies for the quaternization of N(sp^2 and sp^3) n-donor bases (B) with MeI in MeCN at 298 K (reaction i), $\Delta G^{\ddagger}_{MeI}$(MeCN), are linearly related to the standard free energy changes for the gas-phase protonation of the same bases (reaction ii), ΔG_{H^+}(g). These LFERs are compared to those relating ΔG_{H^+}(g) and the standard free energy changes

$$B + CH_3I \xrightarrow{MeCN} BCH^+_3 + I^- \quad (i)$$

$$B(g) + H^+(g) \rightarrow BH^+(g) \quad (ii)$$

for model donor–acceptor reactions in solution. These results shed light on important aspects of the Menshutkin reaction and strongly suggest that, *for processes not involving extensive charge dispersal from the solute to the solvent or strongly specific solvent–solute interactions, gas-phase basicities are the choice reference property for Brønsted analyses.*

Introduction

It has long been recognized[1] that alkylation of N(sp^2) and N(sp^3) n-donor bases (B) by alkyl halides (RX) in solution, a typical Menshutkin reaction[2] (eq 1), is a Lewis acid–base process.

$$B + RX \rightarrow BR^+ + X^- \quad (1)$$

Generalized Brønsted correlations,[3] i.e., linear relationships between the standard free energy change for the protonation of B

† CSIC.
‡ Universidad Autônoma de Barcelona.
§ University of California.

(1) (a) Brown, H. C. *J. Chem. Educ.* **1959**, *36*, 424 and references therein. (b) Brown, H. C. *J. Chem. Soc.* **1956**, 1248.

0002-7863/91/1513-4738$02.50/0